Redox-dependent niche differentiation provides evidence for multiple bacterial sources of glycerol tetraether lipids in lakes

Yuki Weber[a,1,2], Jaap S. Sinninghe Damsté[b,c], Jakob Zopfi[a], Cindy De Jonge[b,3], Adrian Gilli[d], Carsten J. Schubert[e], Fabio Lepori[f], Moritz F. Lehmann[a], and Helge Niemann[a,b,g]

[a]Department of Environmental Sciences, University of Basel, 4056 Basel, Switzerland; [b]Department of Marine Microbiology and Biogeochemistry, Royal Netherlands Institute for Sea Research and Utrecht University, 1790 AB Den Burg, The Netherlands; [c]Faculty of Geosciences, Department of Earth Sciences, Geochemistry, Utrecht University, 3584 CD Utrecht, The Netherlands; [d]Geological Institute, ETH Zurich, 8092 Zurich, Switzerland; [e]Department of Surface Waters - Research and Management, Swiss Federal Institute of Aquatic Science and Technology, 6047 Kastanienbaum, Switzerland; [f]Department for Environment, Constructions and Design, Institute of Earth Sciences, University of Applied Sciences and Arts of Southern Switzerland, 6952 Canobbio, Switzerland; and [g]Centre for Arctic Gas Hydrate, Environment and Climate, Department of Geology, The Arctic University of Norway, 9037 Tromsø, Norway

Edited by Donald E. Canfield, Institute of Biology and Nordic Center for Earth Evolution, University of Southern Denmark, Odense M., Denmark, and approved September 20, 2018 (received for review April 9, 2018)

Terrestrial paleoclimate archives such as lake sediments are essential for our understanding of the continental climate system and for the modeling of future climate scenarios. However, quantitative proxies for the determination of paleotemperatures are sparse. The relative abundances of certain bacterial lipids, i.e., branched glycerol dialkyl glycerol tetraethers (brGDGTs), respond to changes in environmental temperature, and thus have great potential for climate reconstruction. Their application to lake deposits, however, is hampered by the lack of fundamental knowledge on the ecology of brGDGT-producing microbes in lakes. Here, we show that brGDGTs are synthesized by multiple groups of bacteria thriving under contrasting redox regimes in a deep meromictic Swiss lake (Lake Lugano). This niche partitioning is evidenced by highly distinct brGDGT inventories in oxic vs. anoxic water masses, and corresponding vertical patterns in bacterial 16S rRNA gene abundances, implying that sedimentary brGDGT records are affected by temperature-independent changes in the community composition of their microbial producers. Furthermore, the stable carbon isotope composition ($\delta^{13}C$) of brGDGTs in Lake Lugano and 34 other (peri-)Alpine lakes attests to the widespread heterotrophic incorporation of ^{13}C-depleted, methane-derived biomass at the redox transition zone of mesotrophic to eutrophic lake systems. The brGDGTs produced under such hypoxic/methanotrophic conditions reflect near-bottom water temperatures, and are characterized by comparatively low $\delta^{13}C$ values. Depending on climate zone and water depth, lake sediment archives predominated by deeper water/low-^{13}C brGDGTs may provide more reliable records of climate variability than those where brGDGTs derive from terrestrial and/or aquatic sources with distinct temperature imprints.

paleoclimate | lakes | GDGT | $\delta^{13}C$ | microbial ecology

Accurate prediction of future climate depends on our understanding of the present and past climate system. As such, the assessment of paleoclimatic conditions on timescales exceeding instrumental records is indispensable for evaluating the performance of existing climate models. Particularly challenging is the numerical parameterization of the terrestrial climate system, because of the heterogeneous nature of continental environments (1), which underlines the urgent need for paleoclimate data from inland areas. Lake sediments represent the most important type of terrestrial climate archives, because they are widely distributed, provide high temporal resolution due to fast and continuous sedimentation, and contain organic compounds as carriers of paleoclimatic information, which are often well preserved (2).

Molecular fossils such as bacterial tetraether membrane lipids [branched glycerol dialkyl glycerol tetraethers (brGDGTs); Fig. 1] preserved in sediments provide important information on past climate conditions (e.g., ref. 3). These insights into the past are based on the empirical correlation of the brGDGT distribution in contemporary soils with mean annual air temperature (MAT) and pH, which, in turn, gave rise to the hypothesis that brGDGT-producing microbes adjust the composition of their membranes in response to changing environmental conditions (4, 5). This mechanism is known as "membrane lipid homeostasis" (6), and is also pertinent to other molecular proxies such as archaeal tetraether lipids (7). Quantitative links between the brGDGT composition and latitudinal/altitudinal MAT gradients are evident in surface sediments of lakes (8, 9), enabling the reconstruction of past climate variability in lacustrine sedimentary archives, and linking continental paleoclimate records with those from the marine realm (e.g., ref. 10).

Significance

Reliable prediction of future climate conditions requires a thorough understanding of climate variability throughout Earth's history. Microbial molecular fossils, such as bacterial membrane-spanning tetraether lipids [branched glycerol dialkyl glycerol tetraethers (brGDGTs)], have proven to be particularly useful for the assessment of past climatic conditions, because they occur ubiquitously in the environment and show compositional changes related to temperature. However, the identity and ecology of brGDGT-producing bacteria is largely unknown, and a mechanistic basis for brGDGT-based paleoclimate reconstruction is still lacking. Here, we present insights into the ecological parameters that affect brGDGT synthesis in lakes, demonstrating that eutrophic lakes with oxygen-deprived bottom waters are the preferred sites for brGDGT-based reconstructions of continental climate.

Author contributions: J.S.S.D., M.F.L., and H.N. designed research; Y.W. performed research; J.Z., C.D.J., A.G., C.J.S., and F.L. contributed new reagents/analytic tools; Y.W. analyzed data; Y.W. wrote the paper; J.S.S.D., M.F.L., and H.N. advised research; and H.N. oversaw research in his role as principal investigator.

The authors declare no conflict of interest.

This article is a PNAS Direct Submission.

Data deposition: The sequences reported in this paper have been deposited in the GenBank database (accession nos. MH111698–MH113143).

[1]Present address: Department of Earth and Planetary Sciences, Harvard University, Cambridge, MA 02138.

[2]To whom correspondence should be addressed. Email: yuki_weber@fas.harvard.edu.

[3]Present address: Research Group of Plant and Ecosystems, Department of Biology, University of Antwerp, B-2610 Wilrijk, Belgium.

This article contains supporting information online at www.pnas.org/lookup/suppl/doi:10.1073/pnas.1805186115/-/DCSupplemental.

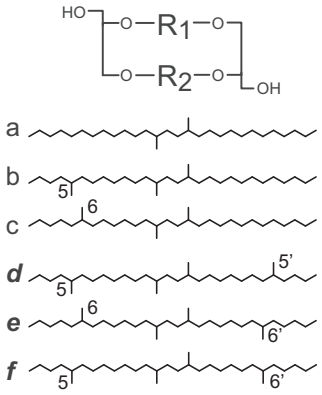

R_1	R_2	brGDGT	isomer
a	a	Ia	—
a	b	IIa	C5
b	b	IIIa	
a	***d***		
a	c	IIa′	C6
c	c	IIIa′	
a	***e***		
b	c	IIIa″	C5/6
a	***f***		

Fig. 1. Structures of the major tetramethylated (Ia), pentamethylated (IIa, IIa′), and hexamethylated (IIIa, IIIa′, IIIa″) brGDGT core lipids, containing dimethyloctacosanes (a), trimethyloctacosanes (b, c), and tetramethyloctacosanes (d, e, f) as the central alkyl moieties (R1, R2). Positions of the peripheral methyl branches are given to denote brGDGT isomer classes, which are referred to as C5-, C6-, and C5/6-methylated brGDGTs. Minor brGDGTs with cyclopentyl moieties are shown in *SI Appendix*, Fig. S1. Note that brGDGTs IIIa, IIIa′, and IIIa″ each comprise a symmetric and an asymmetric isomer that are not distinguishable by liquid chromatography, with the asymmetric ones comprising distinctive alkyl moieties (d, e, and f; boldface italic).

Despite the ubiquitous presence of brGDGTs in both terrestrial and freshwater environments, knowledge of the identity and ecophysiology of their source organisms is still severely limited. The glycerol stereochemistry of brGDGTs in peat revealed that these compounds are produced by bacteria (11), which is remarkable in light of the fact that the vast majority of cultured bacterial strains exclusively contain ester- (instead of ether) bound membrane lipids. The diverse and still poorly characterized Acidobacteria represent an important component of microbial communities in soils and peat bogs (12, 13), and were suggested as potential biological sources because brGDGT abundance correlates with acidobacterial 16S rRNA gene copy numbers (11, 14). So far, only soil-inhabiting members of this phylum have been found to produce building blocks of brGDGTs, i.e., *iso* diabolic acid (and derivatives), whereas full brGDGT structures are largely absent in the available acidobacterial isolates (15). Information on the occurrence and diversity of Acidobacteria in lakes, however, is extremely rare (e.g., refs. 16–18), and potential links between microbial ecology and aquatic brGDGT synthesis are uncertain.

To identify the locus of brGDGT biosynthesis within the water column, and to constrain the ecology of their microbial producers in lakes, we investigated the distribution and stable carbon isotope composition of their alkyl moieties in the water column of Lake Lugano (Switzerland), as well as in surface sediments of 34 other lakes in the European Alps. In Lake Lugano, we further compared the vertical distribution and abundance of bacterial 16S rRNA genes with those of individual brGDGT isomers, and assessed the potential for aquatic brGDGT synthesis by lipid stable isotope probing. We provide conclusive evidence for lacustrine brGDGT production by spatially segregated microbial communities thriving under both oxic and hypoxic/anoxic conditions, and the export of deeper water-derived brGDGTs to the sediments. These insights into the ecology of tetraether lipid-producing bacteria are important for unraveling the biological source(s) of these ubiquitous bacterial lipids, and will allow for a more causative understanding of brGDGT paleo records in lake deposits.

Results and Discussion

Multiple Microbial brGDGT Sources in Lake Lugano. The North Basin of Lake Lugano is 288 m deep, mesotrophic, and meromictic, with a permanent oxycline at ∼100 m and a seasonal thermocline at 10 m to 20 m water depth (Fig. 2*A*). The brGDGT pool in suspended particulate matter (SPM) was dominated by noncyclic hexamethylated brGDGTs comprising three structural isomers (i.e., IIIa, IIIa′, and IIIa″; Fig. 1), which accounted for 46 to 94% of all brGDGTs in the water column (data for the less abundant brGDGTs are shown in *SI Appendix*, Figs. S2 and S3). The organic carbon-normalized total concentration of brGDGTs was low in near-surface waters (∼4 ng·g^{-1} at 10 m depth), but increased to ∼100 ng·g^{-1} just below the thermocline (Fig. 2*B*). Similarly, the fraction of intact polar brGDGTs that still retain the labile head group moieties present in living cells increased with depth from ∼30% at the base of the thermocline to >70% (Fig. 2*B*; see *SI Appendix* for further information). This is consistent with pronounced brGDGT synthesis in the deeper (anoxic) waters of the lake, which has previously been observed in other (seasonally) stratified lake systems (19–21).

We found profound changes in the relative contribution of brGDGTs IIIa, IIIa′, and IIIa″ throughout the water column (Fig. 2*C*). While brGDGT IIIa showed a continuous increase with depth across the redox transition zone (RTZ), IIIa′ was most abundant within oxygenated waters ∼20 m above the oxic–anoxic interface, and rapidly decreased below. In stark contrast to all other brGDGTs, the IIIa″ isomer, which was recently identified in anoxic sediments of another Alpine lake (22), occurred exclusively at depths below 90 m. Moreover, it was detected neither in nearby catchment soils nor in riverbed sediments collected from the lake's watershed (*SI Appendix*, Fig. S5 and Table S1), suggesting that it is exclusively produced by anaerobic bacteria within the deeper waters (cf. ref. 22).

The spatially segregated production of these structurally similar brGDGTs in oxic and hypoxic/anoxic water masses is also reflected in their sinking fluxes, which we assessed by analyzing settling particles collected in sediment traps from three different depths throughout an annual cycle (Fig. 2*C*). Fluxes of IIIa′ increased ∼10-fold between the upper (20 m) and middle (85 m) trap but did not further increase below, indicating that it is predominantly biosynthesized in the lower part of the oxygenated water column. In contrast, IIIa″ was only present in settling particles below the RTZ (176 m), further attesting to its exclusive production within oxygen-deprived waters. IIIa, on the other hand, showed increasing fluxes across the RTZ, suggesting that it is produced by both aerobic and anaerobic, or facultative anaerobic, bacteria.

Distinct sources of these specific brGDGTs within Lake Lugano are also indicated by the stable carbon isotope signature of their alkyl moieties. In contrast to the bulk of brGDGT-derived alkanes that showed significantly decreasing $\delta^{13}C$ values with depth (i.e., up to 10‰; Fig. 2*D*), the C isotope signature of alkane e that is exclusively contained in brGDGT IIIa′ (compare Fig. 1) remained unchanged across the RTZ, suggesting that it is only produced in the oxygenated part of the lake, from where it is exported to the sediment. To further explore the potential of brGDGT biosynthesis under oxic conditions, we amended near-surface SPM from Lake Lugano (10 m depth) with ^{13}C-enriched organic substrates (see *SI Appendix* for details). Indeed, we observed pronounced production of the brGDGT IIIa′ and other C6-methylated isomers, providing evidence for an aerobic metabolism of their producers, whereas IIIa, IIIa″, and all other C5-methylated brGDGTs were not detectable at the end of the experiment (*SI Appendix*, Fig. S6).

The clear vertical segregation of the isomers IIIa′ and IIIa″, as well as their distinct stable carbon isotope signatures, strongly suggests that they are produced by distinct (groups of) microorganisms with different redox requirements. To elaborate links between brGDGT synthesis and microbial niche differentiation, we investigated vertical trends in the bacterial population by 16S rRNA gene sequencing. The change in brGDGT composition across the RTZ was accompanied by a marked shift in the bacterial community, with only 11% of the operational taxonomic units (OTUs) being shared between oxic (10 m to 80 m) and anoxic (90 m to 275 m) water masses. Furthermore, we compared OTU-specific DNA concentrations with the concentration

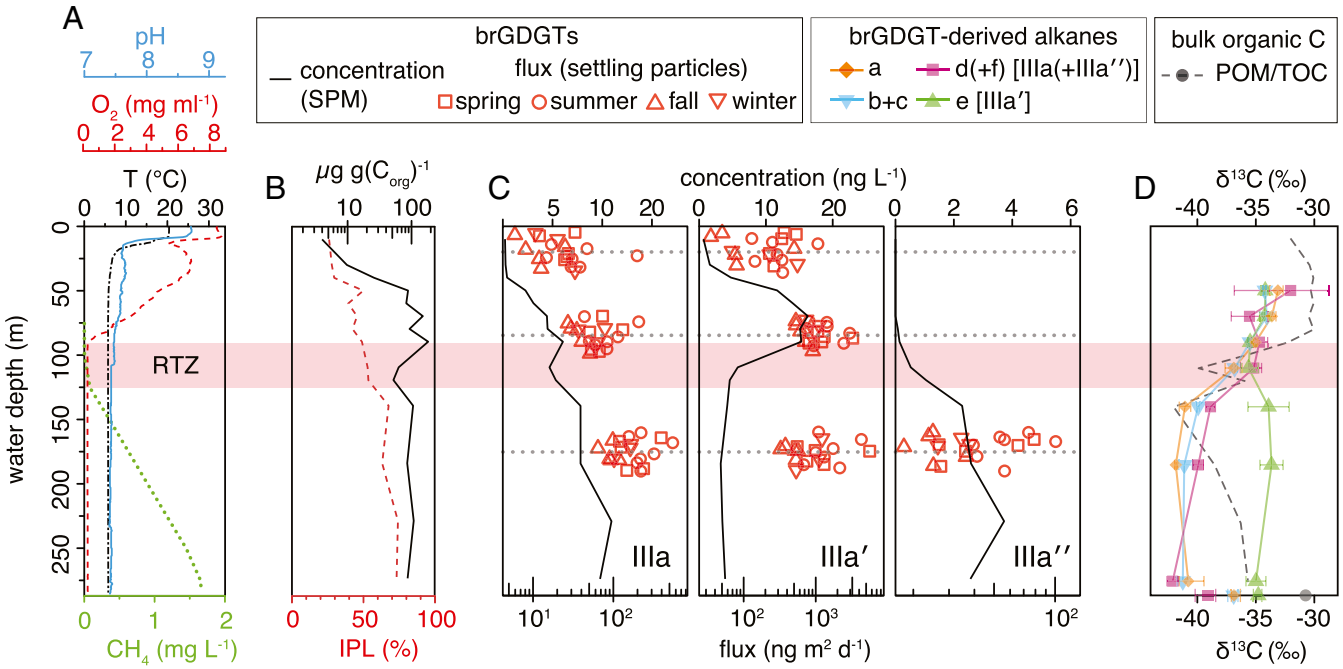

Fig. 2. Redox-dependent segregation and ^{13}C depletion of brGDGTs in Lake Lugano (Switzerland). (*A*) In situ dissolved oxygen (dashed line), dissolved methane (dotted line), water temperature (dot-dashed line), and pH (solid line) in September 2014. The water layer with methanotrophic activity is referred to as the RTZ and highlighted in red. (*B*) Organic carbon (C_{org})-normalized total concentration of brGDGTs (black solid line), as well as the relative contribution of intact polar lipids (IPLs; see *SI Appendix* for further information) to the total brGDGT pool (dashed red line) in suspended particles (SPM) collected in September 2014. (*C*) Total concentration (i.e., sum of intact polar and core brGDGT fractions) of the three predominant brGDGT isomers (IIIa, IIIa′, and IIIa″) in the water column (black solid lines), and corresponding fluxes (open symbols) measured in sediment traps deployed at three discrete depths (dotted horizontal lines) throughout an annual cycle (March 1990 to March 1991). Data for the less abundant brGDGTs are shown in *SI Appendix*, Figs. S2 and S3. Settling particles were sampled up to three times per month, and random vertical jitter was added to reduce overlap of symbols. The analytical error for absolute brGDGT quantification was <±10% (2 SD). (*D*) Stable C isotopic composition of the brGDGTs' alkyl moieties released by ether cleavage (a to f; solid lines), particulate/total organic carbon (POM/TOC; dashed line and circle) in SPM and surface sediment (bottom symbols). Due to incomplete gas chromatographic separation (*SI Appendix*, Fig. S4), peaks of b+c and d+f (if f was present) were integrated as a whole. The characteristic association of alkanes d, e, and f with specific brGDGTs is indicated in square brackets (compare Fig. 1). Isotopic analysis of brGDGTs in SPM from near-surface water (<50 m) was not possible, due to low concentrations. Error bars represent the range of duplicate/triplicate GC-IRMS analyses. The range of replicate $\delta^{13}C_{POM/TOC}$ measurements was <0.2‰.

of each individual brGDGT in the water column (see *SI Appendix* for details). A substantial fraction of the bacterial community (i.e., 30% of the OTUs) showed a strong correlation ($r > 0.75$) with the abundance of at least one of the major brGDGTs, whereas this correlation was much weaker when all brGDGTs were considered as a whole ($r \lesssim 0.5$; *SI Appendix*, Fig. S7). Moreover, the bacterial clades that correlated with individual brGDGTs were often taxonomically distinct from one another (Fig. 3). In particular, the OTUs correlating well with brGDGT IIIa′ had taxonomic affiliations distinct from those corresponding to brGDGTs IIIa″, in support of brGDGT synthesis by multiple (groups of) bacteria that reside in different ecological niches (e.g., oxic vs. hypoxic/anoxic).

Acidobacteria are a plausible biological source of brGDGT, due to their membrane lipid composition (15). In Lake Lugano, 58% of all acidobacterial OTUs correlated well ($r > 0.75$) with one or more of the major brGDGT, and the diversity between the acidobacterial groups associated with different brGDGTs varied strongly (Fig. 3). This attests to a marked niche partitioning among members of the Acidobacteria that seems to resemble the differential vertical trends of certain brGDGTs in the water column (*SI Appendix*, Fig. S8). However, the vertical distribution of brGDGT also corresponded to OTUs belonging to many other bacterial phyla (Fig. 3 and *SI Appendix*, Fig. S7), suggesting that the trait of brGDGT synthesis extends beyond the phylum of Acidobacteria. Because ecological niches within the water column are often shared by diverse groups of microbes due to syntrophic relationships (23) or similar metabolic lifestyles (17), we cannot draw definite conclusions on the identity of brGDGT producers in Lake Lugano.

Carbon Metabolism of brGDGT-Producing Bacteria in Lake Lugano. In Lake Lugano's water column, the ^{13}C content of brGDGTs (assessed by their alkyl moieties) provides insight into the potential C substrates utilized by their bacterial producers. Coinciding with the marked shift in the brGDGT distribution, the ^{13}C content of most brGDGTs (i.e., the $\delta^{13}C$ values of the alkyl moieties a, b, and c) decreased from −33 to −42‰ across the RTZ (Fig. 2*D*). This may, in part, reflect the vertical $\delta^{13}C$ gradient of the C substrate utilized by brGDGT producers, and/or may be due to a distinct biosynthetic ^{13}C fractionation expressed by different (groups of) source organisms. To elucidate this further, we measured ^{13}C in the inorganic and organic C pools that may serve as substrates for brGDGT production within the water column. In fact, bulk suspended particulate organic matter (POM) showed vertical ^{13}C trends similar to the brGDGTs (i.e., a decline across the RTZ; Fig. 2*D*), whereas $\delta^{13}C$ values of dissolved inorganic and dissolved organic C did not change substantially with depth (*SI Appendix*, Fig. S9). We therefore conclude that brGDGT-producing bacteria in Lake Lugano are likely involved in the heterotrophic breakdown and assimilation of particulate organic C in the water column, which is in agreement with the known metabolic capabilities of acidobacterial isolates (24), and analogous to what has previously been suggested for peat bogs and soils (25, 26).

The more negative $\delta^{13}C_{POM}$ values encountered at the RTZ, in turn, are predominantly due to the presence of methanotrophic bacteria that oxidize and incorporate ^{13}C-depleted methane (−60‰) at and below the anoxic interface (27). We thus argue that at least some of the brGDGT producers thriving within the RTZ are part of a methane-based microbial food web (22, 28), in which they assimilate organic matter that is derived either directly from

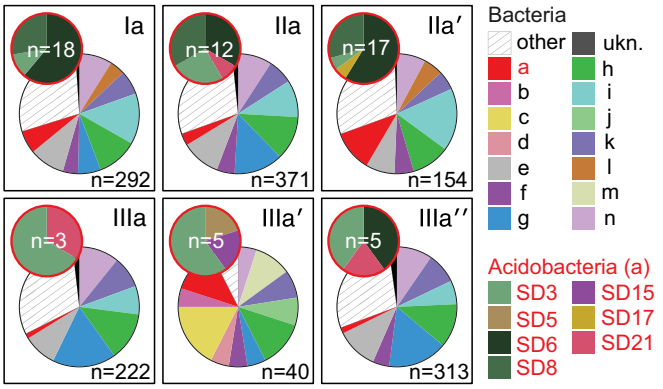

Fig. 3. Diversity of OTUs that show strong empirical correlation ($r > 0.75$) with at least one of the six major brGDGTs in Lake Lugano (30% of all 1,581 OTUs analyzed). OTU-specific DNA concentrations were estimated based on bacterial 16S rRNA gene abundances and total DNA concentrations (see *SI Appendix* for details), and the vertical concentration profiles of OTUs and individual brGDGTs were then compared by bivariate correlation analysis (*SI Appendix*, Fig. S7; https://github.com/yukiweber/phylo.lipids). The phylogenetic affiliation of the highly correlated OTUs ($r > 0.75$) is shown for each brGDGT on the phylum level (large pie charts) and is further differentiated for the Acidobacteria (class level, smaller pie charts, red). The diversity of the (acido) bacteria associated with each brGDGT is markedly distinct, suggesting differential brGDGT synthesis by multiple (acido) bacterial taxa. Key: a, Acidobacteria; b, Actinobacteria; c, Alphaproteobacteria; d, Armatimonadetes; e, Bacteroidetes; f, Betaproteobacteria; g, Chloroflexi; h, Deltaproteobacteria; i, Firmicutes; j, Gammaproteobacteria; k, Planctomycetes; l, Spirochaetae; m, TM6–Dependentiae; n, Verrucomicrobia; ukn., unknown phylum; SD3 to SD21, subdivisions of the Acidobacteria. Phyla contributing less than 4% to the total number of OTUs in each group are subsumed as "other." The number of OTUs in each group (*n*) is shown for each pie chart.

methanotrophic bacteria and/or from other organisms that have previously incorporated methanotroph-derived carbon (29–31).

Methane-Fueled brGDGT Production and Microbial Niche Differentiation in Other Lakes. A redox-dependent differentiation of the brGDGT-producing bacterial community as we observed in meromictic Lake Lugano may be a common feature in other stratified lake systems. Indeed, in 20% of the lake sediments investigated in this study, the characteristic alkyl moiety derived from brGDGT IIIa′ (alkane e) had substantially higher $\delta^{13}C$ values (≥4‰) than those originating from brGDGTs IIIa and IIIa″ (alkanes d and f; Fig. 4*A*). This isotopic offset further seems to be associated with lakes that are more eutrophic and have relatively lower $\delta^{13}C_{d,f}$ values. We therefore assume that the production of brGDGT IIIa′ in these lakes is also spatially separated from that of the bulk of the other major brGDGTs, similar to what we show for Lake Lugano (compare Fig. 2*D*). Moreover, in >50% of the lake sediments, the most common alkyl moieties of brGDGTs (i.e., alkanes a, b, and c) were depleted in ^{13}C relative to total organic carbon (TOC) (i.e., ≥5‰ lower $\delta^{13}C$ values) (Fig. 4*B*), again indicating a substantial contribution of brGDGTs produced in methanotrophic water and/or sediment layers, as we propose for Lake Lugano (see also *SI Appendix*, Fig. S5). Remarkably, these low $\delta^{13}C_{(a,b,c)}$ values are consistently associated with an elevated trophic state of the lake (Fig. 4*C*), which, in turn, gives rise to an enhanced export production, as well as anoxia (Fig. 4*D*) and methane accumulation in bottom waters (32). Eutrophication and redox stratification thus likely promote the growth of brGDGT-producing microbes at the RTZ where methanotrophy may play an important role in microbial food webs. As indicated by the $\delta^{13}C$ data, these deeper water-derived brGDGTs substantially contribute to the sedimentary brGDGT pool.

In Lake Lugano, the production of brGDGT IIIa″ is restricted to hypoxic/anoxic water (compare Fig. 2*C*). Corroboratively, we detected this compound preferentially in sediments of mesotrophic to eutrophic lakes (9 out of 11 cases; *SI Appendix*, Table S1), where biological oxygen consumption is likely to cause anoxia within the bottom water and/or the top layer of the surface sediment. The presence of brGDGT IIIa″ may thus be used as a redox indicator and, indirectly, as a proxy for the trophic state. Taken together, redox-dependent differentiation of brGDGT-producing bacterial communities, as shown here for Lake Lugano, seems to be prevalent in a substantial fraction of lake systems. Compositional shifts in sedimentary brGDGT records may thus not only reflect the ability of bacteria to adapt the chemical properties of their membrane in response to temperature and pH (5, 6), but may also be strongly dependent on changes in the trophic state (33) and the microbial community composition.

Implications for Lacustrine Paleothermometry. Observed correlations between brGDGT distributions in recent lake sediments and MAT gave rise to transfer functions that allow for the quantitative reconstruction of paleoclimatic conditions from lacustrine sediment archives (e.g., ref. 9). For instance, the Methylation Index of brGDGTs (MBT'_{5me}, reflecting the relative amount of C5-methyl branches; ref. 4) has been successfully applied to East African lake sediments, where it showed a strong correlation with MAT ($r = 0.96$; ref. 34). However, this correlation was poor for the surface sediments of the lakes investigated here ($r = 0.33$, $n = 36$). Several factors may affect the fidelity of brGDGT-based temperature proxies in lake sediments. One major concern is that terrigenous brGDGTs may contribute to the sediment through soil organic matter inputs. The brGDGTs from soils have a composition

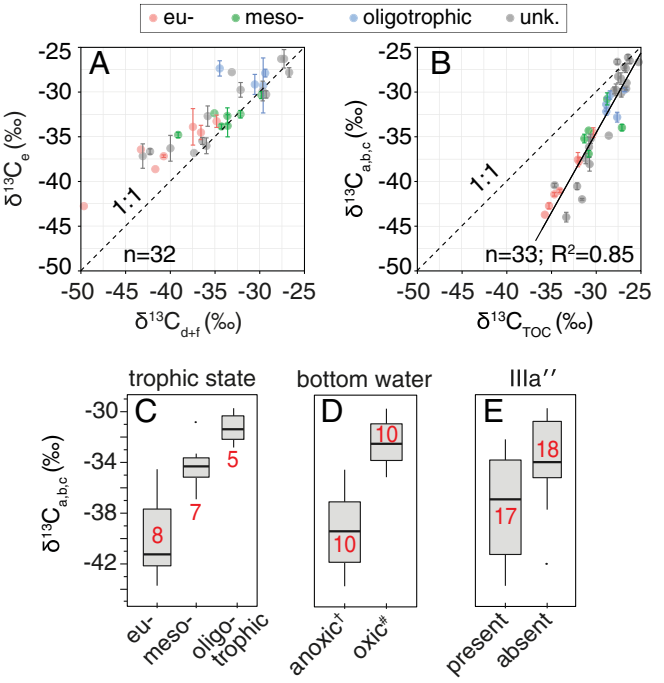

Fig. 4. Stable C isotope composition of brGDGT-derived alkanes (a to f) and TOC in lake surface sediments from the European Alps. (*A*) Alkane e that exclusively originates from brGDGT IIIa′ was up to 7‰ ^{13}C-enriched relative to alkanes d+f derived from IIIa and IIIa″. Average values for d+f are reported because gas chromatographic separation was incomplete (*SI Appendix*, Fig. S4). (*B*) The abundance-weighted average $\delta^{13}C$ values of the most common alkanes a, b, and c ($\delta^{13}C_{a,b,c}$) show a strong correlation with $\delta^{13}C_{TOC}$ (solid line), and were up to 10‰ depleted in ^{13}C relative to TOC. (*C*–*E*) Comparison of $\delta^{13}C_{a,b,c}$ values with trophic state, bottom water oxygenation, and occurrence of brGDGT IIIa″ in lake sediments from the European Alps. Note that water chemistry records are not available for all study sites. Trophic classification is based on epilimnetic total N and/or total P concentrations. Hydrochemical data were provided by the Swiss Federal Office of the Environment, or taken from literature (*SI Appendix*, Table S1); unk., unknown; †, seasonally or permanently anoxic; #, year-round oxic.

that is markedly distinct from those produced within lakes of the same climate regime (8), and, as a consequence, their admixture to the aquatically produced brGDGT pool can substantially bias temperature estimates derived from lake deposits. Another factor relates to the vertical temperature distribution within the water column. Besides a possible input of soil-derived brGDGTs, the water depth from where the in situ-produced brGDGTs are predominantly transferred to the sediments will ultimately determine the "temperature imprint" of brGDGT in the surface sediment. In Lake Lugano, the largest part of the brGDGT sinking flux can be attributed to production in subthermocline (i.e., hypolimnetic) water (compare Fig. 2*C*), and thus the pool of brGDGTs finally reaching the sediment reflects isothermal deeper water, rather than seasonal surface water conditions (refs. 19 and 35 and *SI Appendix*, Fig. S10). On the other hand, in lakes with less-pronounced deeper water production, the sedimentary brGDGTs may more dominantly derive from surface water, shifting the proxy record toward higher temperatures (i.e., increased MBT index values). The relative contributions of soil-, (near) surface water-, and hypolimnion-derived proxy signals to the sediments may consequently vary largely among different study sites, depending on hydrochemical parameters (e.g., trophic state/redox conditions), morphological characteristics (i.e., maximal depth), and the depositional environment (i.e., soil organic matter input), which is likely to confound the quantitative relationships between atmospheric MAT and the sedimentary brGDGT record. Knowledge of the predominant brGDGT sources, therefore, is of prime importance for the use of brGDGTs in paleoenvironmental reconstructions.

Our data from Lake Lugano show that the brGDGTs produced at the RTZ—likely by utilization of methane-derived C compounds—are much more depleted in ^{13}C than those synthesized in both the oxic part of the water column ($\gtrsim$35‰; compare Fig. 2*D*) and soil [−25 to −31‰ (25, 26); see also *SI Appendix*, Table S1]. Such ^{13}C-depleted sedimentary brGDGT pools in eutrophic lakes may thus be indicative of proxy signals that almost exclusively reflect variations in deeper water temperatures, and may hence be largely unaffected by above-mentioned differential brGDGT inputs from surface water and/or soils. To further investigate the temperature response of sediments with a deeper water-dominated brGDGT source, we reassessed the MAT–brGDGT correlation in our dataset for different $\delta^{13}C$ domains. We found that, in mesotrophic to eutrophic lakes with low $\delta^{13}C_{(a,b,c)}$ values (−45 to −36‰), the correlation between MBT'_{5me} (and related proxy indices; *SI Appendix*, Fig. S11) and MAT was indeed significant ($r = 0.67$, $n = 15$, $P < 0.01$), and much stronger than in oligo- to mesotrophic lakes, where the $\delta^{13}C_{(a,b,c)}$ was higher ($r = 0.16$, $n = 20$, $P = 0.5$). This correlation was again substantially improved when only shallow lakes with a maximal depth of <40 m were considered ($r = 0.87$, $n = 10$, $P < 0.01$; Fig. 5*B*), in which the RTZ may overlap with the thermocline, and the low-^{13}C brGDGTs thus probably reflect thermocline water temperatures. In contrast, MBT'_{5me} proxy values were more or less constantly low among the deeper lakes (>40 m) (Fig. 5*D*), which we attribute to the decoupling of atmospheric air and hypolimnetic water temperatures in lakes of the cool-temperate climate zone (i.e., MAT $\lesssim$ 11 °C; ref. 36). In warmer climates, on the other hand, the temperature of hypolimnetic water is, in fact, linearly related to that of the atmosphere (37, 38), and hypolimnion-derived brGDGTs from deeper lakes will therefore be more responsive to interannual MAT variations than in the Alpine lakes investigated here.

We thus conclude that deeper water communities of brGDGT-producing bacteria thriving at the RTZ "reset" the sedimentary brGDGT "thermometer" to (near-)bottom water temperature, thereby mitigating the interfering effects of surface water- and/or catchment soil-derived brGDGT signatures. Depending on climate zone and water depth, such settings, which can be identified by the C isotopic imprint of brGDGTs inherited from biogenic methane, are expected to yield reliable records of climate variability, and are preferable sites for the application of brGDGT-based paleotemperature proxies in lakes.

Materials and Methods

Water Column Sampling. SPM was collected from Lake Lugano (northern basin) close to the deepest location (*SI Appendix*, Fig. S12) in September 2014 by large-volume in situ filtration of lake water (~50–300 L), using a double layer of glass fiber (GF) filters (2.7 and 0.7 μm; Whatman GF/D and GF/F). The filters were frozen on dry ice immediately after sampling and stored at −80 °C until further processing. Settling particles were collected at the same location, using cylindrical sediment traps (d = 10 cm) deployed in 1990/1991 at three depths (20, 85, and 176 m), and were sampled up to three times per month.

Sampling of Sediments and Soils. Lake surface sediments (*SI Appendix*, Fig. S13 and Table S1) were obtained by gravity coring during multiple field campaigns (2008 to 2014). The core tops (upper ~5 cm) were then subsampled, homogenized, and freeze-dried before extraction. We further collected eight to ten top-soil samples (0 cm to 10 cm) within a perimeter of ~500 m at 19 of the 36 investigated lakes. The individual soil samples from each lake site were pooled, freeze-dried, sieved (2 mm), and homogenized with a mortar before extraction. Additionally, we collected sediment samples (0 cm to 10 cm) from two main tributaries (Cuccio and Casarate) of Lake Lugano at locations close to the river mouths (*SI Appendix*, Fig. S12), which were processed in the same way as the soil samples.

Lipid Extraction. Sediments and soils were extracted three times by accelerated solvent extraction (ASE300; Thermo Fisher Scientific) (5). For SPM samples, we employed a sequential solvent extraction and acid hydrolysis procedure to assure complete recovery of brGDGTs from living cells (intact polar brGDGTs; see also *SI Appendix*), and to avoid losses and biases associated with modified Bligh–Dyer extraction (39). Briefly, the freeze-dried SPM was extracted by ultrasonication with methanol and dichloromethane as solvents, and the residual material was subsequently subjected to acid hydrolysis. To maximize lipid recovery for compound-specific stable C isotope analysis of brGDGTs, SPM from selected depths (representing ~150 L of filtered water) was subjected to acid hydrolysis before ultrasonic solvent extraction.

brGDGT Analysis. The brGDGT-containing lipid fractions were prepared as previously described (39), spiked with an internal standard (40), and analyzed by ultra-high-performance liquid chromatography (UHPLC) positive ion atmospheric pressure chemical ionization mass spectrometry in selected ion monitoring mode. For all samples from Lake Lugano, analytical separation of GDGTs was achieved using two UHPLC columns in series (ACQUITY UPLC BEH HILIC, 130 Å, 1.7 μm, 2.1 mm × 150 mm; Waters) (41), whereas, for all remaining sites, we used an array of four HPLC columns (Alltima Silica, 100 Å, 3 μm, 2.1 mm × 150 mm; W. R. Grace & Co.) (4). Both "high-resolution" UHPLC setups reliably separate C5- and C6-methylated brGDGT isomers (41). Response was monitored regularly using a known mixture of the internal standard and crenarchaeol.

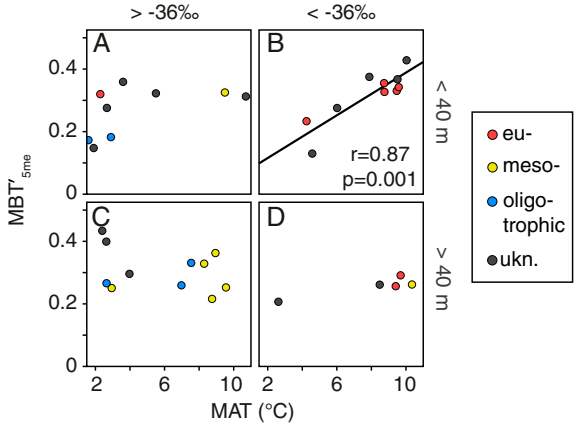

Fig. 5. Lapse rate-based MAT of the study sites plotted against the brGDGT proxy MBT'_{5me} (Methylation Index of C5-methylated brGDGTs) in lake surface sediments from the European Alps (n = 35). Sites are binned by maximum water depth (*A*, *B* vs. *C*, *D*) and the approximated average stable C isotope composition of brGDGTs ($\delta^{13}C_{a,b,c}$; *A*, *C* vs. *B*, *D*). A regression line is only shown for models with significant slope coefficients ($P < 0.02$). Related brGDGT proxy indices are shown in *SI Appendix*, Fig. S11.

Stable C Isotope Analyses. The $\delta^{13}C$ content of TOC and POM were determined after acidification of the sample (42) by elemental analysis followed by isotope ratio mass spectrometry (IRMS) (22). For stable carbon isotope analysis of brGDGTs, we subjected bulk brGDGT fractions to ether cleavage (57% HI), and measured $\delta^{13}C$ values of the released alkyl moieties by gas chromatography combustion (GC/C) IRMS as previously described (22), with a few modifications (*SI Appendix*).

Molecular Biological Methods. DNA was extracted from fractions of GF filters (43), equivalent to 2 L to 7 L of lake water. A two-step PCR approach (Nextera; Illumina Corp.) was employed for library preparation, using the universal primers 515F-Y (5′-GTGYCAGCMGCCGCGGTAA) and 926R (5′-CCGYCAATTYMTTTRAGTTT-3′) (44) that target the V4 and V5 regions of the 16S rRNA gene. The individual samples were indexed, pooled at equimolar concentrations, and sequenced on an Illumina MiSeq V2 platform using the 2×250 bp paired-end protocol (Microsynth Inc.). After initial quality control and bioinformatical processing (*SI Appendix*), taxonomy was assigned to OTUs by comparison with the SILVA 128 SSU reference database (https://www.arb-silva.de/documentation/release-128/). To compare vertical trends of brGDGTs and microbial taxa, relative OTU abundances were converted to OTU-specific DNA concentrations (nanograms per liter) by multiplication with the total amount of extracted DNA, and subsequently subjected to correlation analysis in R (see *SI Appendix* for details).

Data Access and Availability. Abundance-filtered 16S rDNA sequences are deposited at GenBank (National Center for Biotechnology Information) under accession numbers MH111698 through MH113143. Raw bacterial OTU abundances are provided in Dataset S1. The brGDGT data from Lake Lugano and other Alpine lake sediments and catchment soils are included in Dataset S2. R code for correlation analysis is available at https://github.com/yukiweber/phylo.lipids.

ACKNOWLEDGMENTS. We thank Marco Simona and Stefano Beatrizotti for logistics and equipment for lake sampling, and Ellen Hopmans, J. Ossebaar, and Thomas Kuhn for analytical support in the laboratory. This research was funded by the Swiss National Science Foundation Grants SNF 200021_140662 and 200020_162414 and by the European Research Council under the European Union's Horizon 2020 Research and Innovation Programme Grant Agreement 694569 – MICROLIPIDS. J.S.S.D. received further funding for this work through the Netherlands Earth System Science Centre and through gravitation Grant NWO 024.002.001 from the Dutch Ministry for Education, Culture and Science.

1. Gettelman A, Rood RB (2016) *Demystifying Climate Models* (Springer, Berlin).
2. Castañeda IS, Schouten S (2011) A review of molecular organic proxies for examining modern and ancient lacustrine environments. *Quat Sci Rev* 30:2851–2891.
3. Fawcett PJ, et al. (2011) Extended megadroughts in the southwestern United States during Pleistocene interglacials. *Nature* 470:518–521.
4. De Jonge C, et al. (2014) Occurrence and abundance of 6-methyl branched glycerol dialkyl glycerol tetraethers in soils: Implications for palaeoclimate reconstruction. *Geochim Cosmochim Acta* 141:97–112.
5. Weijers JWH, Schouten S, van den Donker JC, Hopmans EC, Sinninghe Damsté JS (2007) Environmental controls on bacterial tetraether membrane lipid distribution in soils. *Geochim Cosmochim Acta* 71:703–713.
6. Zhang YM, Rock CO (2008) Membrane lipid homeostasis in bacteria. *Nat Rev Microbiol* 6:222–233.
7. Schouten S, Forster A, Panoto FE, Sinninghe Damsté JS (2007) Towards calibration of the TEX86 palaeothermometer for tropical sea surface temperatures in ancient greenhouse worlds. *Org Geochem* 38:1537–1546.
8. Tierney JE, et al. (2010) Environmental controls on branched tetraether lipid distributions in tropical East African lake sediments. *Geochim Cosmochim Acta* 74:4902–4918.
9. Pearson EJ, et al. (2011) A lacustrine GDGT-temperature calibration from the Scandinavian Arctic to Antarctic: Renewed potential for the application of GDGT-paleothermometry in lakes. *Geochim Cosmochim Acta* 75:6225–6238.
10. Loomis SE, Russell JM, Lamb HF (2015) Northeast African temperature variability since the Late Pleistocene. *Palaeogeogr Palaeoclimatol Palaeoecol* 423:80–90.
11. Weijers JWH, et al. (2006) Membrane lipids of mesophilic anaerobic bacteria thriving in peats have typical archaeal traits. *Environ Microbiol* 8:648–657.
12. Weijers JWH, et al. (2009) Constraints on the biological source(s) of the orphan branched tetraether membrane lipids. *Geomicrobiol J* 26:402–414.
13. Jones RT, et al. (2009) A comprehensive survey of soil acidobacterial diversity using pyrosequencing and clone library analyses. *ISME J* 3:442–453.
14. Peterse F, Nicol GW, Schouten S, Sinninghe Damsté JS (2010) Influence of soil pH on the abundance and distribution of core and intact polar lipid-derived branched GDGTs in soil. *Org Geochem* 41:1171–1175.
15. Sinninghe Damsté JS, et al. (2018) An overview of the occurrence of ether- and ester-linked iso -diabolic acid membrane lipids in microbial cultures of the Acidobacteria: Implications for brGDGT paleoproxies for temperature and pH. *Org Geochem* 124:63–76.
16. Zimmermann J, Portillo MC, Serrano L, Ludwig W, Gonzalez JM (2012) Acidobacteria in freshwater ponds at Doñana National Park, Spain. *Microb Ecol* 63:844–855.
17. Preheim SP, et al. (2016) Surveys, simulation and single-cell assays relate function and phylogeny in a lake ecosystem. *Nat Microbiol* 1:16130.
18. Parfenova VV, Gladkikh AS, Belykh OI (2013) Comparative analysis of biodiversity in the planktonic and biofilm bacterial communities in Lake Baikal. *Microbiology* 82:91–101.
19. Buckles LK, Weijers JWH, Verschuren D, Sinninghe Damsté JS (2014) Sources of core and intact branched tetraether membrane lipids in the lacustrine environment: Anatomy of Lake Challa and its catchment, equatorial East Africa. *Geochim Cosmochim Acta* 140:106–126.
20. Hu J, Zhou H, Peng P, Spiro B (2016) Seasonal variability in concentrations and fluxes of glycerol dialkyl glycerol tetraethers in Huguangyan Maar Lake, SE China: Implications for the applicability of the MBT-CBT paleotemperature proxy in lacustrine settings. *Chem Geol* 420:200–212.
21. Woltering M, et al. (2012) Vertical and temporal variability in concentration and distribution of thaumarchaeotal tetraether lipids in Lake Superior and the implications for the application of the TEX 86 temperature proxy. *Geochim Cosmochim Acta* 87:136–153.
22. Weber Y, et al. (2015) Identification and carbon isotope composition of a novel branched GDGT isomer in lake sediments: Evidence for lacustrine branched GDGT production. *Geochim Cosmochim Acta* 154:118–129.
23. Liu J, et al. (2014) Molecular characterization of a microbial consortium involved in methane oxidation coupled to denitrification under micro-aerobic conditions. *Microb Biotechnol* 7:64–76.
24. Kielak AM, Barreto CC, Kowalchuk GA, van Veen JA, Kuramae EE (2016) The ecology of Acidobacteria: Moving beyond genes and genomes. *Front Microbiol* 7:744.
25. Weijers JWH, Wiesenberg GLB, Bol R, Hopmans EC, Pancost RD (2010) Carbon isotopic composition of branched tetraether membrane lipids in soils suggest a rapid turnover and a heterotrophic life style of their source organism(s). *Biogeosciences* 7:2959–2973.
26. Pancost RD, Sinninghe Damsté JS (2003) Carbon isotopic compositions of prokaryotic lipids as tracers of carbon cycling in diverse settings. *Chem Geol* 195:29–58.
27. Blees J, et al. (2014) Micro-aerobic bacterial methane oxidation in the chemocline and anoxic water column of deep south-Alpine Lake Lugano (Switzerland). *Limnol Oceanogr* 59:311–324.
28. Colcord DE, Pearson A, Brassell SC (2017) Carbon isotopic composition of intact branched GDGT core lipids in Greenland lake sediments and soils. *Org Geochem* 110:25–32.
29. Sinninghe Damsté JS, et al. (1995) Evidence for gammacerane as an indicator of water column stratification. *Geochim Cosmochim Acta* 59:1895–1900.
30. Guhl BE, Finlay BJ (1993) Anaerobic predatory ciliates track seasonal migrations of planktonic photosynthetic bacteria. *FEMS Microbiol Lett* 107:313–316.
31. Stock M, et al. (2013) Exploration and prediction of interactions between methanotrophs and heterotrophs. *Res Microbiol* 164:1045–1054.
32. Blees J, et al. (2014) Bacterial methanotrophs drive the formation of a seasonal anoxic benthic nepheloid layer in an alpine lake. *Limnol Oceanogr* 59:1410–1420.
33. Tierney JE, Schouten S, Pitcher A, Hopmans EC, Sinninghe Damsté JS (2012) Core and intact polar glycerol dialkyl glycerol tetraethers (GDGTs) in Sand Pond, Warwick, Rhode Island (USA): Insights into the origin of lacustrine GDGTs. *Geochim Cosmochim Acta* 77:561–581.
34. Russell JM, Hopmans EC, Loomis SE, Liang J, Sinninghe Damsté JS (2017) Distributions of 5- and 6-methyl branched glycerol dialkyl glycerol tetraethers (brGDGTs) in East African lake sediment: Effects of temperature, pH, and new lacustrine paleotemperature calibrations. *Org Geochem* 117:56–69.
35. Colcord DE, et al. (2015) Assessment of branched GDGTs as temperature proxies in sedimentary records from several small lakes in southwestern Greenland. *Org Geochem* 82:33–41.
36. Butcher JB, Nover D, Johnson TE, Clark CM (2015) Sensitivity of lake thermal and mixing dynamics to climate change. *Clim Change* 129:295–305.
37. Straile D, Jöhnk K, Rossknecht H (2003) Complex effects of winter warming on the physicochemical characteristics of a deep lake. *Limnol Oceanogr* 48:1432–1438.
38. Vollmer MK, et al. (2005) Deep-water warming trend in Lake Malawi, East Africa. *Limnol Oceanogr* 50:727–732.
39. Weber Y, Sinninghe Damsté JS, Hopmans EC, Lehmann MF, Niemann H (2017) Incomplete recovery of intact polar glycerol dialkyl glycerol tetraethers from lacustrine suspended biomass. *Limnol Oceanogr Methods* 15:782–793.
40. Huguet C, et al. (2006) An improved method to determine the absolute abundance of glycerol dibiphytanyl glycerol tetraether lipids. *Org Geochem* 37:1036–1041.
41. Hopmans EC, Schouten S, Sinninghe Damsté JS (2016) The effect of improved chromatography on GDGT-based palaeoproxies. *Org Geochem* 93:1–6.
42. Whiteside JH, et al. (2011) Pangean great lake paleoecology on the cusp of the end-Triassic extinction. *Palaeogeogr Palaeoclimatol Palaeoecol* 301:1–17.
43. Deiner K, Walser JC, Mächler E, Altermatt F (2015) Choice of capture and extraction methods affect detection of freshwater biodiversity from environmental DNA. *Biol Conserv* 183:53–63.
44. Parada AE, Needham DM, Fuhrman JA (2016) Every base matters: Assessing small subunit rRNA primers for marine microbiomes with mock communities, time series and global field samples. *Environ Microbiol* 18:1403–1414.